IEEE Access
Multidisciplinary ⋮ Rapid Review ⋮ Open Access Journal

Received October 20, 2020, accepted November 16, 2020, date of publication November 20, 2020,
date of current version December 8, 2020.

Digital Object Identifier 10.1109/ACCESS.2020.3039516

Crash Risk-Based Prioritization of Basic Safety Message in DSRC

SEUNGMO KIM[1], (Member, IEEE), AND BYUNG-JUN KIM[2]
[1]Department of Electrical and Computer Engineering, Georgia Southern University, Statesboro, GA 30460, USA
[2]Department of Mathematical Sciences, Michigan Technological University, Houghton, MI 49931, USA

Corresponding author: Seungmo Kim (seungmokim@georgiasouthern.edu)

This work was supported by the Georgia Department of Transportation (GDOT) under Grant RP 20-03.

ABSTRACT Dedicated short-range communications (DSRC) is one of the key technologies enabling safety-critical applications for intelligent transportation system (ITS). Considering the significance of such safety-of-life applications, it is of utmost importance to guarantee reliable delivery of basic safety messages (BSMs). However, in accordance with a V2X network being inherently dynamic in key aspects such as vehicle density and velocity, the networking behavior of a DSRC system is usually highly complicated to analyze. In addition, the United States Federal Communications Commission (US FCC) recently proposed the so-called "5.9 GHz band innovation," which includes a plan to reduce bandwidth for DSRC to 10 MHz at best from 75 MHz. Motivated from these challenges, the necessity of "lightening" load of a DSRC network has become essential to keep safety-related operations from performance deterioration. To this end, this paper proposes a protocol that prioritizes transmission of a BSM from a vehicle according to the level of accident risk of the vehicle. The proposed protocol uses the distance of a vehicle from a danger source as the metric to determine the priority for transmission. Our results show that this protocol effectively prioritizes the transmission opportunity for dangerous vehicles, and hence results in higher performance in terms of key metrics–i.e., average latency, packet delivery rate (PDR), and inter-reception time (IRT).

INDEX TERMS V2X, IEEE 802.11p, DSRC, message prioritization, 5.9 GHz band.

I. INTRODUCTION

A. MOTIVATION

Vehicle-to-Everything (V2X) communications have been garnering massive interest across the academic and commercial bodies thanks to their potential to significantly promote the traffic safety [1]. As such, the technologies take a central role in constitution of safety-critical applications in intelligent transportation system (ITS) and connected vehicle networks. Today, two major radio access technologies (RATs) enabling V2X communications have been attracting particular research interest: namely, Dedicated Short-Range Communications (DSRC) and cellular V2X (C-V2X). In 1999, the United States Federal Communications Commission (US FCC) allocated DSRC to the 5.9 GHz band (viz., 5.850-5.925 GHz). Recently, however, C-V2X has been proposed to operate in the same band along with cellular operators' licensed bands [2].

Of the two RATs, DSRC has longer been deployed in many communities for as the key enabler technology for safety-critical applications owing to several merits. First, DSRC is a mature technology that has already been tested and deployed by a wide variety of stakeholders including car manufacturers and state governments in various aspects including not only technology but practical domains such as policy and deployment preparations [3]. Second, DSRC does not require any paid subscription, which makes possible wider deployment at a lower cost [3]. Third, the universal compatibility among IEEE 802.11 technologies leads to the spectrum versatility and easy operation [4], which could strengthen DSRC in the market of connected vehicles.

Based on these advantages, as of November 2018, more than 5,315 roadside units (RSUs) operating in DSRC were deployed in the United States (US) alone [5]. In December 2016, the US National Highway Traffic Safety Administration (NHTSA) proposed to mandate DSRC for all new light vehicles [6]. However, despite the advantages and widespread deployment, the technology has encountered an unprecedented obstacle: the *5.9 GHz band reallocation* by the US FCC [7].

In December 2019, the US FCC voted to allocate the lower 45 MHz (i.e., 5.850-5.895 GHz), out of entire 75 MHz of the 5.9 GHz band (i.e., 5.850-5.925 GHz), for unlicensed operations to support high-rate broadband applications

The associate editor coordinating the review of this manuscript and approving it for publication was Oussama Habachi.

(e.g., Wireless Fidelity, or Wi-Fi) [7]. While the reallocation is proposing to leave the upper 30 MHz (i.e., 5.895-5.925 GHz) for ITS operations (viz., DSRC and C-V2X), it is also proposing to dedicate the upper 20 MHz of the chunk (i.e., 5.905-5.925 GHz) for C-V2X.

Therefore, according to this plan, DSRC is only allowed to use 10 MHz of spectrum (i.e., 5.895-5.905 GHz) at maximum. It has *never been studied nor tested if 10 MHz would suffice* for operation of the existing DSRC-based transportation safety infrastructure. Many states in the US have already invested large amounts of fortune in the deployment of connected vehicle infrastructure based on DSRC [8]. As such, it has become urgent to understand how much impact of the FCC's 5.9 GHz band reallocation will be placed on the performance of such connected vehicle infrastructure.

Another significant issue for DSRC is that it may need to experience coexistence with C-V2X users according to the FCC's proposition [7]. The key technical challenge here is that the C-V2X standards adopt significantly different protocols, which makes the technology incompatible with DSRC-based operations. In fact, based on the author's recent investigation [9], DSRC may be severely interfered by C-V2X if the two disparate technologies coexist in a *co-channel* basis. Therefore, it has become crucial to lighten the load of a DSRC network while keeping the dissemination of packets operable, in order to suit the technology into such a competitive spectrum environment.

B. CONTRIBUTIONS

As shall be detailed in Section II, the current literature shows a key limitation to achieve the load lightening of a DSRC network: despite being a predominant factor determining the performance of a V2X network, the length of backoff time was allocated to each vehicle without considering ''semantic'' contexts that the vehicle is experiencing.

We would regard it more efficient from the system's point of view if vehicles being closer to a danger take higher chances to transmit. The rationale is that these vehicles in the closest proximity of a danger-causing object are the key nodes in the network for expedited propagation of basic safety messages (BSMs). That is, the other vehicles in the network will be able to receive the BSMs only after those being close to the danger source have successfully transmitted the BSMs.

To this line, this paper proposes a V2X networking scheme where a vehicle takes a transmission opportunity according to *the distance to a danger source*. Moreover, we clearly distinguish our contributions from the most relevant work [11]. While the prior work focused on the stochastic geometry of a particular coexistence scenario between military and civilian vehicles in an urban area, this present paper significantly extends the scope of discussion to (i) a general two-dimensional geometry and (ii) detailed analysis on networking behaviors–viz., an exact backoff allocation method.

Overall, the technical contributions of this paper distinguished from the literature can be summarized as follows:

1) It proposes a method prioritizing a BSM according to the level of danger to which each vehicle is exposed.
2) In order to measure the danger, it uses the ''distance to a danger source,'' which is a quantity that is easy to obtain by using the existing techniques and apparatus.
3) Based on (i) key metrics–namely, latency, packet delivery rate (PDR), and IRT–and (ii) a generalized two-dimensional spatial model (not limited to certain road models), it provides a stochastic analysis framework characterizing a DSRC network's broadcast of BSMs.

II. RELATED WORK

A. PERFORMANCE ANALYSIS SCHEMES

1) MATHEMATICAL ANALYSIS FRAMEWORK

Analysis frameworks based on stochastic geometry for DSRC have been provided recently [9]– [12]. They commonly rely on the fact that uniform distributions of nodes on X and Y axes of a Cartesian-coordinate two-dimensional space yield a Poisson point process (PPP) on the number of nodes in the space [13]. This paper distinguishes itself from the prior proposals in the sense that it applies the stochastic geometry framework for analysis of the temporal aspect of DSRC multiple access mechanisms.

2) PERFORMANCE EVALUATION METHOD

A recent proposal combines a packet-level simulation model with data collected from an actual vehicular network [14]. It is critical to discuss the potential impacts of *internal* and *external* bandwidth contentions, which form a critical discussion point after the US FCC's recent 5.9 GHz band reallocation [7]. The ''internal'' contention means the contention among DSRC vehicles themselves, while the ''external'' contention refers to the contention incurred by other RAT(s).

The limitation of the prior art lies in that the performance evaluation was performed without consideration of these bandwidth contentions, which might undermine its own generality. For instance, it is assumed that (i) safety messages and (ii) packets for non-safety applications are sent over separate DSRC channels [14], whereby no interference is generated between safety and Internet traffic. This assumption has become obsolete according to the US FCC's recent proposition where DSRC may not be able to utilize multiple channels any more [7].

3) CONGESTION IN DSRC NETWORKS

It has been found that a DSRC network is constrained by packet expirations (EXPs) and collisions over the air [36]. An *EXP* refers to a packet ''drop'' as a result of not being able to (i) make it through the backoff process and hence (ii) be transmitted within a beaconing period. Since the IEEE 802.11p broadcast of BSMs does not support retry nor acknowledgement (ACK), an expired packet is dropped and the next packet with a new sequence number is generated [31]– [33]. The reason of a packet not being able to go through a backoff process is finding the medium busy, which hinders the backoff counter from being decremented.

Meanwhile, a *collision* is composed of two types of cause: a synchronized transmission (SYNC) or a hidden node (HN).

The performance of a DSRC broadcast system in a high-density vehicle environment has been studied [16], yet the assumption was too ideal to be realistic, which means that the number of vehicles within a vehicle's communication range was kept constant. Another study proposed a DSRC-based traffic light control system [17], but it limited the applicability to the traffic lights only.

4) SAFETY-RELATED APPLICATION

Furthermore, we concentrate on DSRC's networking to support the safety-critical applications. In the related literature, a DSRC-based end of queue collision warning system has been proposed [18]. However, it discusses a one-dimensional freeway model, which needs significant improvement for application to an intersection with two or more ways.

5) EXTERNAL BANDWIDTH CONTENTION

Lastly, the objective of our proposed protocol is to lighten the traffic load of a DSRC network to better suit in an environment of coexisting with a disparate technology (viz., C-V2X) according to the 5.9 GHz reallocation [7]. The performance degradation of DSRC under interference from Wi-Fi has been studied [19]; however, it lacks consideration of coexistence with C-V2X.

B. PERFORMANCE IMPROVEMENT SCHEMES

Various modifications on the binary exponential backoff (BEB) algorithm have been proposed as a means to improve throughput and fairness in general carrier-sense multiple access (CSMA) in IEEE 802.11-related technologies. Specifically, adjustment of the contention window (CW) was often suggested to improve the performance of a vehicular communications network such as a recent work [20]. More directly relevant to our work, a distance-based routing protocol has been found to perform better in vehicular ad-hoc networks (VANETs) [21]. Also, in a general ad-hoc network, reduction of the length of a header can be a solution that is worth considering [22]; however, due to a centralized network structure, it shows a limit to be applied to a V2X network. A "subjective" user-end experience optimization is also worth consideration [23], wherein a one-bit user satisfaction indicator was introduced, which served as the objective function in a non-convex optimization.

Another method is the enhanced distributed channel access (EDCA), which divides the data to four queues according to priority: viz., voice, video, best effort and background. Using the default parameter values for EDCA protocol will lead to increasing the collisions in the wireless network and decreasing the capacity [15]. More importantly, such application-specific differentiation of backoff counters cannot be directly applied to the situation that we are targeting to address. That is, we are trying to differentiate the backoff length according to the danger level of each vehicle, instead of the type of application. This makes a compelling case that urgent BSMs for safety-critical use cases need a more dedicated type of networking protocol than the existing EDCA. In this context, this paper proposes a protocol that guarantees to prioritize a BSM with a high urgency.

TABLE 1. Frequently used abbreviations.

Abbreviation	Description
BEB	Binary exponential backoff
BSM	Basic safety message
CAT	Category of distance from danger, $d_{\rightarrow \mathrm{dgr}}$
CSMA	Carrier-sense multiple access
C-V2X	Cellular V2X
CW	Contention window
dgr	The danger source (See Figure 1)
DSRC	Dedicated Short-Range Communications
EXP	Packet expiration
FCC	US Federal Communications Commission
HN	Collision by hidden node
IRT	Inter-reception time
ITS	Intelligent transportation system
ppd	The "proposed" backoff scheme
PPP	Poisson point process
STA	Station
SYNC	Collision by synchronized transmission
tdl	The "traditional" BEB scheme
V2X	Vehicle-to-everything communications

TABLE 2. Key notations.

Notation	Description (unit)
$d_{\rightarrow \mathrm{dgr}}$	Distance of a vehicle to the danger source (m)
λ	Vehicle density (vehicles/m^{-2})
$\mathsf{N}_{\mathrm{bcn}}$	Number of beaconing periods with failed packet delivery (EA)
N_{bo}	Number of slots spent during a backoff process (EA)
$\mathsf{N}_{\mathrm{sta}}$	Number of STAs competing for the medium (EA)
PDR	Packet delivery rate
τ	Probability of a transmission
T_{bo}	Time length taken for a backoff process (sec)
$\mathsf{T}_{\mathrm{col}}$	Time length taken for a packet collision (sec)
$\mathsf{T}_{\mathrm{exp}}$	Time length taken for a packet expiration (sec)
$\mathsf{T}_{\mathrm{ibi}}$	Time length of the inter-broadcast interval (sec)
$\mathsf{T}_{\mathrm{suc}}$	Time length taken for a successful packet delivery (sec)
Th_i	Threshold on $d_{\rightarrow \mathrm{dgr}}$ for CAT i (m)

III. SYSTEM MODEL

This section describes the system model that this paper adopts for analysis. Note that Table 1 lists key abbreviations that are frequently used throughout this paper. Also, mathematical notations are summarized in Table 2.

A. GEOMETRY

A two-dimensional space $\mathbb{R}^2$ is defined as a 2 km-by-2 km square, as illustrated in Figure 1. Once a vehicle reaches the end of the space, it bounces back into the space. This assumption is to maintain a fixed vehicle density and, hence, a same level of competition for the medium at any given time.

The distribution of the nodes follows a *homogeneous PPP* in $\mathbb{R}^2$. We define a general situation where a safety-critical application disseminates BSMs over a V2X network [24]. That is, a source of "danger" exists (expressed as a large black square in Figure 1), which should be avoided by all the other vehicles. The danger source is located at the origin, i.e., the center of $\mathbb{R}^2$. It is noteworthy that the danger source is not expected to generate BSMs to inform the surrounding vehicles; rather, the vehicles approaching this danger source *autonomously detects* it. This assumption is practical based on the fact that a vehicle is likely equipped with various

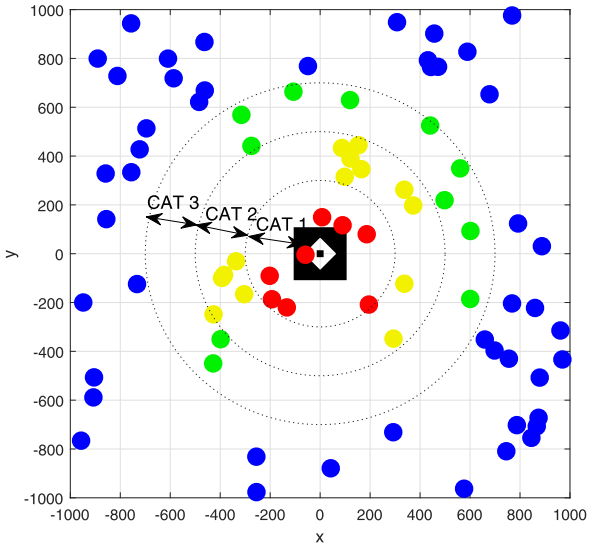

FIGURE 1. An example drop of nodes on $\mathbb{R}^2$ (with the danger source at the origin, $\lambda = 20$ km^{-2}, CAT 1: $0 \leq d_{\rightarrow \text{dgr}} \leq \text{Th}_1$, CAT 2: $\text{Th}_1 < d_{\rightarrow \text{dgr}} \leq \text{Th}_2$, CAT 3: $\text{Th}_2 < d_{\rightarrow \text{dgr}} \leq \text{Th}_3$ where $\{\text{Th}_1, \text{Th}_2, \text{Th}_3\} = \{300, 500, 700\}$ m).

technologies (such as radar, lidar, etc.) enabling the vehicle to detect presence of a hazard. This way, any type of danger source can be detected even including those not being capable of transmitting BSMs, e.g., a construction site, wrecked vehicle, etc.

As shall be detailed in Section IV, our proposed algorithm prioritizes transmission of a BSM as a vehicle is closer to this danger source. This necessitates to measure the *distance from the danger*, which is denoted by $d_{\rightarrow \text{dgr}}$. Figure 1 demonstrates an example "drop" of vehicles with the density of $\lambda = 20$ km^{-2}, which is equivalent to 80 nodes over the defined space $\mathbb{R}^2$. The crash risk is quantified in categories (CATs) according to $d_{\rightarrow \text{dgr}}$ as follows:

$$\begin{aligned} &\text{CAT 1 ("Most dangerous") : } 0 \leq d_{\rightarrow \text{dgr}} \leq \text{Th}_1 \\ &\text{CAT 2 ("Less dangerous") : } \text{Th}_1 < d_{\rightarrow \text{dgr}} \leq \text{Th}_2 \\ &\text{CAT 3 ("Far less dangerous") : } \text{Th}_2 < d_{\rightarrow \text{dgr}} \leq \text{Th}_3 \end{aligned} \quad (1)$$

In Figure 1, vehicles positioned within CATs 1, 2, and 3 are marked as red, yellow, and green circles, respectively. The vehicles that are sufficiently far and thus do not belong to any of the CATs are drawn as blue circles. As shall be depicted in Section IV, the proposed protocol does not allocate these vehicles not belonging to any of the three CATs. The rationale behind this is that these farthest located vehicles are within communications ranges of those belonging to CAT 3. That is, once vehicles in CAT 3 become able to transmit, the messages can be disseminated to these even further vehicles.

Notice, though, that the categorization into three CATs is only an example as an effort to show how the proposed protocol works. In other words, there could be a larger or smaller number of chunks than three; also, the values for each threshold can be set to any values to yield larger or smaller granularity. It means that, although this paper uses three CATs determined by $\{\text{Th}_1, \text{Th}_2, \text{Th}_3\} = \{300, 500, 700\}$ m as an example, the idea proposed in this paper can be extended to other numbers of CATs and other values for thresholds.

B. COMMUNICATIONS

We suppose that all the vehicles distributed in $\mathbb{R}^2$ have the same ranges of carrier sensing and communication. Also, each vehicle broadcasts a BSM every 100 msec, which is denoted by T_{ibi}–i.e., 10 Hz of the broadcast rate. Notice that we assume a BSM to be transmitted within a 50-msec control channel (CCH) according to the multi-channel operation defined by IEEE 1609.4 [25].

We remind that DSRC adopts distributed coordination function (DCF) as the basic access mechanism [26]. This paper assumes that the DCF operates in a saturated-throughput scenario [27]. The purpose of this assumption is to analyze a worst-case scenario (i.e., the heaviest possible network load), which can provide a conservative guideline for the performance evaluation of the proposed scheme in a DSRC network.

It is significant to note that the above-mentioned categorization into CATs 1-3 is mapped to categorization of backoff values, which is the central idea of the mechanism that is proposed in this paper. See Figure 2 for details of the mapping. We reiterate that the three-way categorization is only an example, while the idea can be extended to any other number of categories in terms of $d_{\rightarrow \text{dgr}}$ (and hence CW as well).

Lastly, in accordance with the FCC's 5.9 GHz reallocation [7], this paper assumes the bandwidth of 10 MHz based on the operation in CCH as mentioned earlier.

IV. PROPOSED ALGORITHM

We propose a protocol that controls priority of a packet transmission according to $d_{\rightarrow \text{dgr}}$ as a means to improve the performance of safety-critical messaging in DSRC. This section describes details of the proposed protocol.

1) KEY IMPROVEMENT FROM CONVENTIONAL CSMA

It has been noted that for contention resolution, the conventional BEB algorithm relies on the number of unsuccessful transmission attempts and Physical Layer (PHY)-related factors including packet retry limit, maximum and minimum values of CW size, header format, etc. [28]. This specifically means that once the PHY-specific values are fixed, the future course of the BEB algorithm would be dictated by the number of unsuccessful attempts taken by a STA to successfully transmit the packet. In fact, the PHY parameters will likely remain constant since the current version of IEEE 802.11p does not support a link adaptation [34], [35].

We got motivated from a simple but critical curiosity: why must it be a *uniform* probability to choose a backoff time for all Txs competing for the medium? In other words, in the current CSMA scheme, if there are 50 vehicles on the road at a certain time instant and if they try to transmit a packet at the same time, all of them have an equal opportunity to choose for a backoff time randomly from a range of [0, CW-1]. That is, a vehicle chooses a backoff time in a random manner

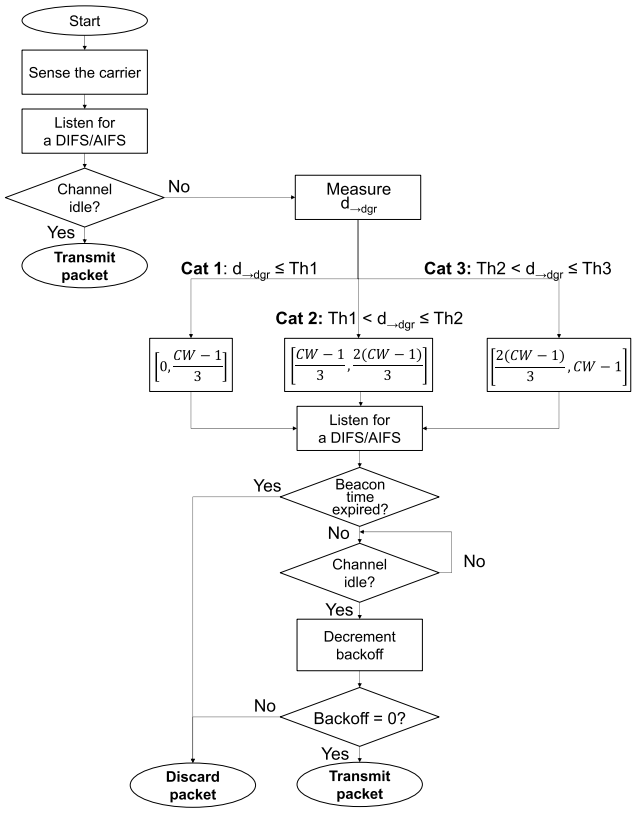

FIGURE 2. Flowchart for the proposed algorithm.

regardless of the level of danger that the vehicle marks. For instance, the Tx STA being far away from a danger source (and thus at a lower risk of a crash) can be allocated a shorter backoff time compared to one being exposed to a higher risk. As an effort to make the protocol more efficient, we propose an idea of assigning a backoff time depending on $d_{\rightarrow \mathrm{dgr}}$, the distance between a STA and the danger source. Specifically, a Tx STA with a smaller $d_{\rightarrow \mathrm{dgr}}$ (i.e., closer to the danger source) will have a shorter backoff time and vice versa.

2) DISTANCE CALCULATION METHOD

One significant discussion regarding the proposed algorithm is the rationale for $d_{\rightarrow \mathrm{dgr}}$ as the metric measuring the risk of a crash. While an accident can be caused by many factors including weather condition, road surface status, mechanical failures, etc., the dominating factor is the inborn reactive time limitation of the drivers [29]. This makes it reasonable to consider the distance to a danger source as a key factor of an accident [30].

Furthermore, one understands that at the current level of technologies, it is not a difficult task to obtain a vehicle's exact distance from a danger source. Specifically, (i) each BSM contains information of the position of its transmitter vehicle based on commercially available techniques such as Global Positioning System (GPS); (ii) in this way, each vehicle is able to exchange each other's exact position; (iii) as such, each vehicle is able to calculate the distance from each other.

3) BACKOFF ALLOCATION ACCORDING TO $d_{\rightarrow \mathrm{dgr}}$

Now, based on the aforementioned rationale, we propose *a backoff allocation algorithm according to the distance to a danger*. A flowchart for the proposed mechanism is provided in Figure 2. Unlike the traditional BEB scheme, *the proposed protocol allocates a smaller backoff to the group of vehicles with a smaller* $d_{\rightarrow \mathrm{dgr}}$. Specifically, according to the threshold distance, Th_i, the vehicles in $\mathbb{R}^2$ are grouped in three categories–viz., CATs 1, 2, and 3. A smaller CAT categorizes a smaller $d_{\rightarrow \mathrm{dgr}}$, which, in turn, means a more urgent need for transmission.

Here is an elaboration on the relationship between CATs and CW. As presented in Section VI, this paper uses {300, 500, 700} m for $\{\mathrm{Th}_1, \mathrm{Th}_2, \mathrm{Th}_3\}$, representing the thresholds defining CATs 1, 2, and, 3, respectively, as have been shown in (1). The proposed protocol divides the entire range of CW into three chunks: for $\{\mathrm{Th}_1, \mathrm{Th}_2, \mathrm{Th}_3\}$, the backoff counter ranges of [0, (CW-1)/3], [(CW-1)/3, 2(CW-1)/3], and [2(CW-1)/3, CW-1] are allocated. Via this modification, a Tx STA belonging to CAT 1, which is at a higher crash risk due to a smaller $d_{\rightarrow \mathrm{dgr}}$, has a higher probability of packet transmission only after a shorter backoff time. In contrast, a STA with a larger $d_{\rightarrow \mathrm{dgr}}$ is designed to hold a bit longer before a transmission.

V. PERFORMANCE ANALYSIS

This section formulates three metrics to measure the performance of the proposed backoff allocation scheme–namely, average latency, PDR, and IRT.

It is worth to notice that all the three quantities are defined with a BSM transmitted at a *tagged vehicle*. We emphasize that such an assumption keeps generality since the type of network being considered in this paper is *distributed*, in which every node has an equal characteristic and hence shows a consistent networking behavior.

A. AVERAGE LATENCY

We remind that this paper focuses on safety-critical applications, which makes the latency as one of the most significant metrics in the performance evaluation of a DSRC network. Further, reflecting the "broadcast" nature of a DSRC network, this paper defines an *average latency* among all the STAs across a network.

Let T denote an instantaneous total latency taken for a node to transmit a packet. Considering all possible results of a packet transmission (viz., expiration, success, and collision), an average latency can be computed as

$$\begin{aligned}\mathbb{E}[\mathsf{T}] &= (1-\mathbb{P}[\mathrm{Tx}])\,\mathbb{T}[\mathrm{Expiration}] \\ &\quad + \mathbb{P}[\mathrm{Tx}]\left\{\mathbb{T}[\mathrm{Success}] + \mathbb{T}[\mathrm{Collision}]\right\} \\ &= (1-\tau)\,\mathbb{E}[\mathsf{T}_{\mathrm{exp}}] \\ &\quad + \tau\left[\mathbb{E}[\mathsf{T}_{\mathrm{bo}}] + \mathbb{E}[\mathsf{T}_{\mathrm{suc}}] + \mathbb{E}[\mathsf{T}_{\mathrm{col}}]\right] \\ &= (1-\tau)\,\mathbb{E}[\mathsf{T}_{\mathrm{exp}}] \\ &\quad + \tau\left[\mathbb{E}[\mathsf{T}_{\mathrm{bo}}] + (1-\mathsf{P}_{\mathrm{col}})\,\mathsf{T}_{\mathrm{suc}} + \mathsf{P}_{\mathrm{col}}\mathsf{T}_{\mathrm{col}}\right] \end{aligned} \quad (2)$$

where $\mathbb{P}[\cdot]$ and $\mathbb{T}[\cdot]$ denote the probability and the time length of an event, respectively. Variables in (2) are defined as follows: τ denotes the probability that a tagged vehicle is able to transmit in a certain slot within a beaconing period [9]; P_{col} gives the probability of a collision–viz., a SYNC or a HN [9]; T_{exp}, T_{col}, and T_{suc} denote the time lengths taken for an expiration, a collision (viz., SYNC and/or HN), and a successful delivery, respectfully.

Proof of (2): Each term in (2) is elaborated as follows:

$\boxed{(1-\tau)\,\mathbb{E}\left[\mathsf{T}_{\text{exp}}\right]}$: We remind that τ is the probability of a tagged vehicle being able to (i) make it through a backoff process before expiration and thus (ii) transmit a packet. For calculation of τ, we modified a Markov chain for the DSRC backoff process [27] in order to reflect the impacts of *packet expiration*, which does not occur in classical IEEE 802.11 DCF and hence was not reflected in the existing analysis models for DCF. Due to a long recursiveness in the computation process, it was more efficient to take a numerical approach to obtain τ instead of a closed-form derivation.

As shown in (3) below, $\mathbb{E}\left[\mathsf{T}_{\text{exp}}\right]$ is meant to express the average time length until a packet successfully completes a backoff process. Notice that the number of consecutive idle beaconing periods, N_{bcn}, can be characterized as a *geometric random variable* [27]. An EXP is modeled as a geometric random variable since it can be abstracted as a "binary" result about whether the packet was able to complete a backoff process within a beaconing period. Therefore, an average time taken for an expiration can be calculated as

$$\begin{aligned}\mathbb{E}[\mathsf{T}_{\text{exp}}] &= (\text{Length of a beaconing period}) \\ &\quad \cdot (\text{Number of beaconing periods spent for EXPs}) \\ &= \mathbb{T}[\text{Beacon}]\,\mathbb{E}\left[\mathsf{N}_{\text{bcn}}\right] \\ &= \mathsf{T}_{\text{ibi}} \cdot (1-\tau)\,\tau^{-1} \end{aligned} \tag{3}$$

where T_{ibi} denotes a beaconing interval (also known as "inter-broadcast interval" or IBI), and $(1-\tau)\tau^{-1}$ gives the mean of a geometric random variable with a success probability of τ in each trial.

$\boxed{\mathbb{E}\left[\mathsf{T}_{\text{bo}}\right] + (1-\mathsf{P}_{\text{col}})\,\mathsf{T}_{\text{suc}}}$: The second term in (2) gives the length of time that is taken for a successfully delivered packet. We start derivation from computing the length of time taken for a backoff, which is given by

$$\mathbb{E}\left[\mathsf{T}_{\text{bo}}\right] = \mathsf{T}_{\text{slot}}\mathbb{E}\left[\mathsf{N}_{\text{bo}}\right] \tag{4}$$

where T_{slot} is the length of a slot [27] (i.e., 66.7 μsec [9]).

Also, in (4), N_{bo} denotes the number of slots spent to go through a backoff process. This quantity can be displayed as a function of the number of STAs, denoted by N_{sta}. Notice that mathematical details for this quantity is given in Section V.C of [36]. We found that N_{bo} does not act as a significant factor in determination of $\mathbb{E}\left[\mathsf{T}_{\text{bo}}\right]$. Yet, here we report two noteworthy tendencies: (i) the proposed scheme consumes a smaller N_{bo} as compared to the traditional CSMA, thanks to higher possibility of shorter backoffs; and (ii) a larger CW spends a larger N_{bo} due to higher possibility of longer backoffs.

Regarding T_{suc} in (2), the number of slots that are used by a successful delivery of a packet is formulated as

$$\begin{aligned}\mathsf{T}_{\text{suc}} &= (\text{Time for a BSM}) \\ &= \text{Hdr} + \text{Pld} + \text{SIFS} + \mathsf{T}_{\text{prop}} \end{aligned} \tag{5}$$

where Hdr and Pld denote the lengths of a header and a payload, respectively. Also, T_{prop} gives the propagation delay, which is assumed to be kept the same to all of the Rx vehicles within the tagged vehicle's communication range.

$\boxed{\mathsf{P}_{\text{col}}\mathsf{T}_{\text{col}}}$: Now, upon transmission with the probability of τ, one needs to examine whether a packet survives from a collision. There are two types of packet collision: namely, SYNC and HN. A SYNC occurs when more than one vehicles happen to start a transmission in an exactly same time slot. The assumption is that although the vehicles are in each other's carrier-sense range, they were unable to sense each other because they coincide to start in the same time slot. A HN occurs among vehicles being unable to sense each other. As such, the probability of a collision is formulated as

$$\begin{aligned}&\mathsf{P}_{\text{col}} \\ &= \mathbb{P}\left[\text{SYNC only}\right] + \mathbb{P}\left[\text{HN only}\right] + \mathbb{P}\left[\text{Both SYNC and HN}\right] \\ &= \mathsf{P}_{\text{sync}}\,(1-\mathsf{P}_{\text{hn}}) + \mathsf{P}_{\text{hn}}\left(1-\mathsf{P}_{\text{sync}}\right) + \mathsf{P}_{\text{sync}}\mathsf{P}_{\text{hn}}. \end{aligned} \tag{6}$$

Mathematical details and proofs for P_{sync} and P_{hn} are found in [36].

See Figure 5 in Section VI for demonstration of P_{col} between the proposed scheme (i.e., CAT 1) and the traditional CSMA. As inferred from Figure 1, the key reason that the proposed scheme achieves a lower P_{col} is a dramatically smaller number of competing nodes.

Now, T_{col} gives the time length that has been taken while going through a collision. One most important note in DSRC is that there is no feedback from a receiver about a packet transmission. It means that no matter it was a SYNC or a HN or both, a vehicle needs to spend an entire transmission cycle, which is formulated as $\mathsf{T}_{\text{col}} \approx \mathsf{T}_{\text{suc}}$. ■

B. PACKET DELIVERY RATE

Another metric that we use to assess the performance of the proposed scheme is PDR, which can be formally written as [36]

$$\begin{aligned}\text{PDR} &= \mathbb{P}\left[\text{Tagged STA transmits}\right]\mathbb{P}\left[\text{No collision}\right] \\ &= \tau\,(1-\mathsf{P}_{\text{col}}) \end{aligned} \tag{7}$$

where P_{col} has been defined in (6). Also, τ has been mentioned after derivation of (2) as well.

C. INTER-RECEPTION TIME

Lastly, we define the IRT as the time taken between two given successful packet reception events. Notice that the unit of a quantity of IRT is "the number of beaconing periods." As such, one can multiply a beaconing time (e.g., 100 msec in this paper) when wanting to display an IRT in the unit of time (i.e., seconds).

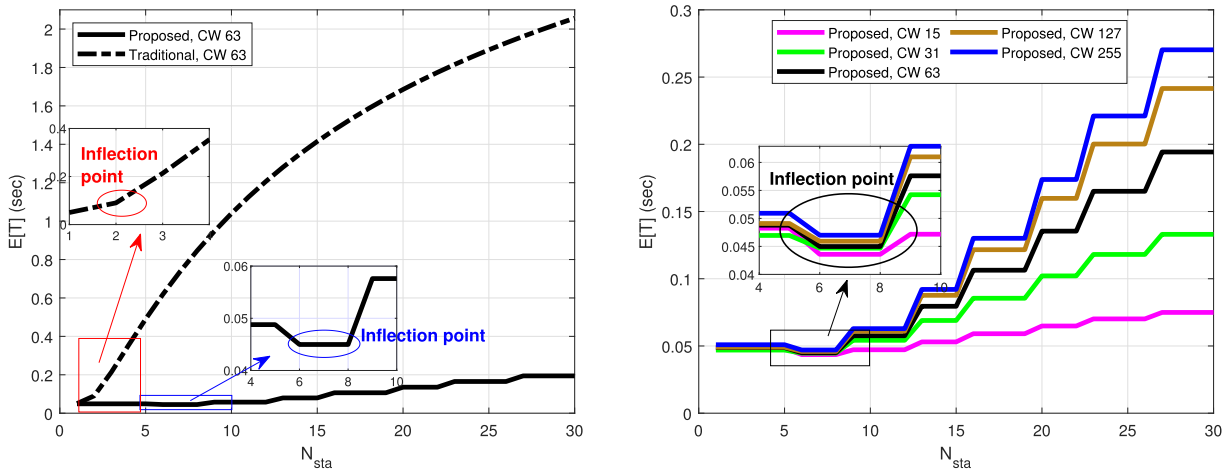

(a) Between proposed and traditional schemes (CAT 1 with CW = 63) (b) According to CW

FIGURE 3. Average latency vs. number of STAs.

TABLE 3. Values for key parameters.

Parameter (Symbol)	Value
Inter-broadcast interval (I_{ibi})	100 msec
DIFS	128 μsec
SIFS	28 μsec
Payload length (Pld)	40 bytes [24]
Propagation delay (T_{prop})	1 μsec
Slot time (T_{slot})	50 μsec
RTS	300 μsec
ACK	300 μsec
CTS	350 μsec
Space size ($\lvert\mathbb{R}^2\rvert$)	2 km by 2 km
CAT threshold distance ($\{\text{Th}_1, \text{Th}_2, \text{Th}_3\}$)	{300, 500, 700} m

Now, the probability that N_{bcn} failures follow a successful delivery is modeled to follow a geometric distribution, which can be formally written as

$$\mathbb{P}\left[\mathsf{IRT} = \mathsf{N}_{\text{bcn}}\right] = (1 - \mathsf{PDR})^{\mathsf{N}_{\text{bcn}}-1}\,\mathsf{PDR}. \tag{8}$$

Proof of (8): For formulation of an "IRT," we start from a successful reception, and then measure how many beaconing periods are expended until the next successful reception. That is, the first beaconing period is set to have the probability of PDR, and thereafter the possibility is left open between PDR and $1 - \mathsf{PDR}$ depending on occurrence of a successful delivery or a failure, respectfully. ■

VI. NUMERICAL RESULTS

In this section, we evaluate the performance of the proposed backoff algorithm compared to the traditional CSMA (i.e., BEB) [26]. As summarized in Table 3, each Tx STA is assumed to have a fixed payload length of 40 bytes [24]. Also, for our numerical analysis, we set the spatial setting being consistent with what was shown in Figure 1.

One thing to note commonly in Figures 3 through 6 is that, regardless in the proposed or the traditional CSMA, the performance of a DSRC network predominantly depends on a packet's (i) EXP and (ii) collision over the air (viz., SYNC and/or HN). This justifies that we ignore impacts of small-scale link-level fluctuations such as Rayleigh and Nakagami fading.

It is noteworthy that plots representing the proposed scheme in Figures 3 through 6 are "stepped" rather than smooth. It is because of rounding the number of STAs to the nearest integer for calculation of binomial coefficients between the number of all STAs and the number of CAT 1 STAs, i.e., "$\mathsf{N}_{\text{sta}}^{\text{all}}$ choose $\mathsf{N}_{\text{sta}}^{\text{cat 1}}$" in calculation of τ. (Notice that the rounding comes from A (CAT 1) / $\lvert\mathbb{R}^2\rvert$ where $\mathsf{A}(\cdot)$ denotes the area of a space.) As such, all the subsequent quantities–viz., τ, P_{col} and PDR–are also affected by the approximation since they are based on τ. See (3) for the relationship between $\mathbb{E}\left[\mathsf{T}_{\text{exp}}\right]$. Meanwhile, see Section V.D of [36] for derivations of P_{col} and PDR in terms of τ.

A. AVERAGE LATENCY

Figure 3 demonstrates the average length of time taken for successful reception of a packet, $\mathbb{E}\left[\mathsf{T}\right]$, versus the number of STAs, N_{sta}, according to the CAT and CW. We remind from (2) that $\mathbb{E}\left[\mathsf{T}\right]$ is composed of three parts: i.e., (i) time taken for an EXP, (ii) that for a successful packet transmission and reception, and (iii) that for a successful packet transmission but a collision. It means that, as N_{sta} grows, all of the three quantities increase, which results in a higher $\mathbb{E}\left[\mathsf{T}\right]$. This relationship is shown in (i) both traditional and proposed schemes as Figure 3a presents and (ii) commonly on all CW sizes as Figure 3b depicts.

The key rationale of the proposed protocol's outperformance is higher τ as displayed in Figure 4a. While it entails a negative margin compared to the traditional scheme in terms of P_{col} as shown in Figure 5, the positive margin from τ is larger and, as a consequence, yields the outperformance in $\mathbb{E}\left[\mathsf{T}\right]$.

The same rationale is behind the positive coupling between $\mathbb{E}\left[\mathsf{T}\right]$ and N_{sta} with respect to CW size, which is described in Figure 3b: a smaller CW size favors in terms of $\mathbb{E}\left[\mathsf{T}\right]$ in spite of disfavor in terms of P_{col}'s.

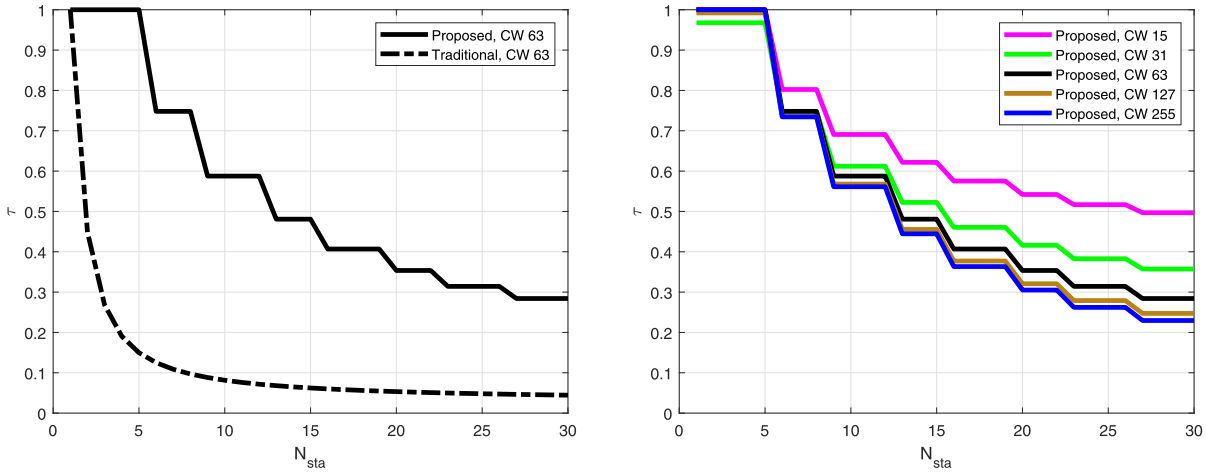

(a) Between proposed and traditional schemes (CAT 1 with CW = 63) (b) According to CW

FIGURE 4. Probability of packet transmission vs. number of STAs.

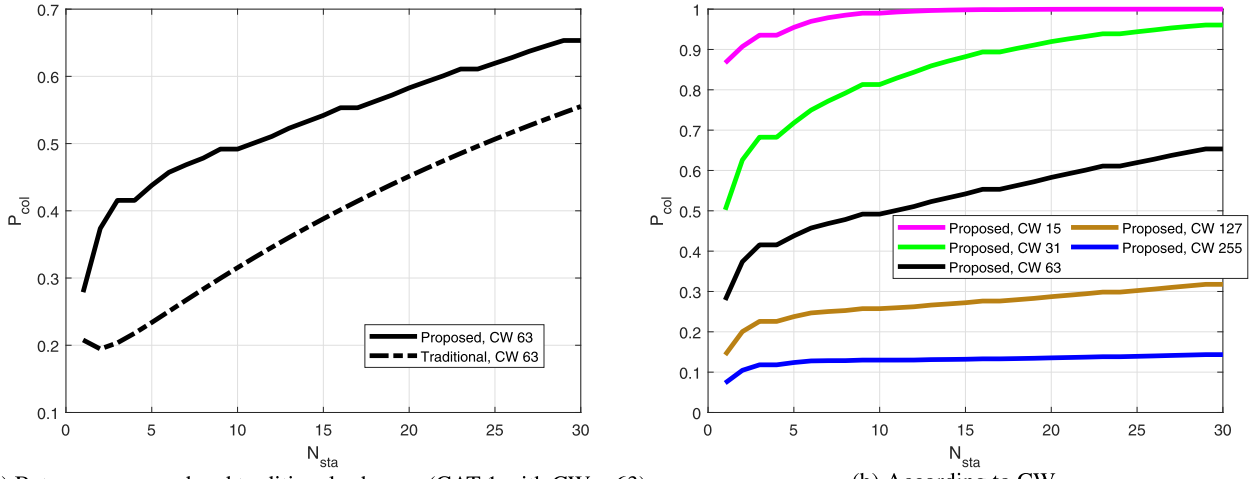

(a) Between proposed and traditional schemes (CAT 1 with CW = 63) (b) According to CW

FIGURE 5. Probability of collision vs. number of STAs.

Although slight, each curve in Figures 3a and 3b shows an inflection point that transitions from a downtrend to an uptrend. It is interesting to observe the downtrend since it means $\mathbb{E}[\mathsf{T}]$ decreases as N_{sta} increases, which is against one's normal intuition. Soon enough, however, the tendency is reversed back to form an upward trajectory, and proceeds to increasing further thereafter. The quantitative rationale is given as below:

- Although not explicitly displayed in the figure, we discovered that initially (i.e., with $\mathsf{N}_{\text{sta}} \approx 0$), $\mathsf{T}_{\text{exp}} \ll \mathsf{T}_{\text{bo}} + \mathsf{T}_{\text{suc}} + \mathsf{T}_{\text{col}}$ and the weight for $\mathsf{T}_{\text{bo}} + \mathsf{T}_{\text{suc}} + \mathsf{T}_{\text{col}}$ is greater than that for T_{exp} since τ is large with a small N_{sta}, as shown in Figure 4.
- Soon after, with N_{sta} being still relatively small, we found that while still $\mathsf{T}_{\text{exp}} < \mathsf{T}_{\text{bo}} + \mathsf{T}_{\text{suc}} + \mathsf{T}_{\text{col}}$, T_{exp} grows far faster than $\mathsf{T}_{\text{bo}} + \mathsf{T}_{\text{suc}} + \mathsf{T}_{\text{col}}$. Now, the weight for T_{exp} is greater than that for the other since τ gets smaller due to N_{sta} being greater.
- Eventually, however, with N_{sta} being large enough, both the quantity and weight get bigger in $\mathsf{T}_{\text{exp}} > \mathsf{T}_{\text{bo}} + \mathsf{T}_{\text{suc}} + \mathsf{T}_{\text{col}}$ and $(1-\tau) > \tau$ as τ gets far smaller due to N_{sta} getting very large.

B. PACKET DELIVERY RATE

Our next metric, PDR, also depends dominantly on τ and P_{col} as shown in (7). Refer to Figures 4 and 5 for understanding the result displayed in Figure 6.

Figure 4 presents τ, the probability that a STA transmits in an arbitrary slot within a beaconing period L_{bcn}, versus the number of STAs competing for the medium, N_{sta}. The figure provides two-fold comparisons: (i) between the proposed and traditional schemes and (ii) according to CW.

Figure 4a does the former: it compares τ between the proposed and traditional CSMA schemes for the most dangerous vehicles (i.e., CAT 1 from Figure 1) with CW = 63. It is straightforward that a larger N_{sta} causes a lower τ. Also, the level of τ is significantly improved in the proposed scheme in comparison to the traditional CSMA. It highlights the principle of the proposed scheme: vehicles being closer to a danger source take higher chances of transmissions in a

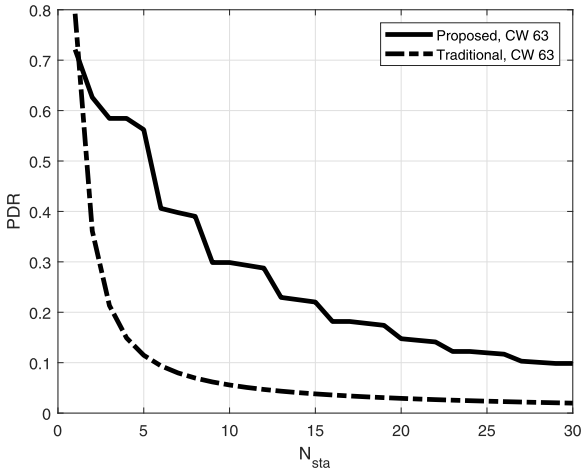

(a) Between proposed and traditional schemes (CAT 1 with CW = 63)

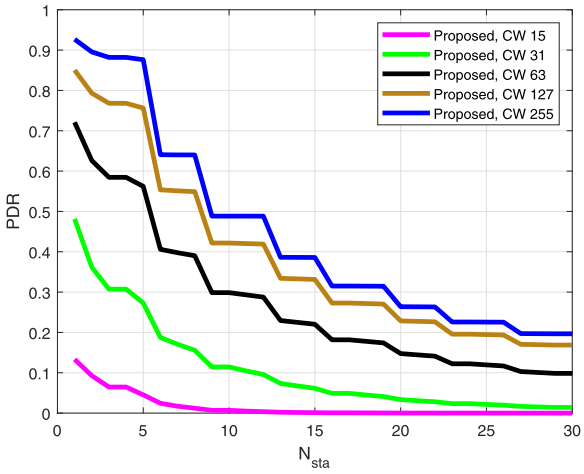

(b) According to CW

FIGURE 6. PDR **vs. number of STAs.**

backoff process. As such, the *semantic message prioritization* is accomplished, which this paper's proposition aims at.

Figure 4b compares τ according to CW. Commonly with the proposed and traditional schemes, a larger CW results in a lower τ due to a longer backoff process. From this, one can infer that the EXP is one of the main causes limiting the performance of a DSRC network.

Now, Figure 5 presents that two-fold comparisons on the other key factor for PDR: the probability of collision, P_{col}.

It is interesting to observe the *downside* of the proposed scheme in Figure 5a: the result shows that the proposed scheme yields a higher P_{col}. It is inevitable because the proposed scheme allows vehicles to transmit a packet with a higher probability by letting them succeed through a backoff process more easily. Also, one can obviously observe that a larger N_{sta} yields a higher P_{col}.

Figure 5b gives a comparison among different CW sizes. It matches one's intuition that a larger CW size yields a lower P_{col} since the STAs can be distributed on a wider window of backoff counter values. This tendency is common in both proposed and traditional schemes.

As a result of the observations of τ and P_{col}, we can demonstrate PDR as shown in Figure 6. We remind from (7) that PDR is directly proportional to τ, which yields that Figure 6 shows a similar overall tendency to what Figure 4 did. Meanwhile, it is critical to understand that the proposed scheme yields higher PDRs compared to the traditional scheme, despite higher P_{col}s. The reason is, as observed from Figures 4 and 5, positive margins in τ being larger than negative margins in P_{col}.

C. INTER-RECEPTION TIME

Figure 7 presents the probability mass function (PMF) and cumulative distribution function (CDF) of random variable N_{bcn}, respectfully, versus N_{sta}. Each row of two subfigures demonstrates a different CW size.

We reiterate that an IRT represents the average length of time that is spent between two successful BSM receptions. As such, the results displayed in Figure 7 translate to the probability that a vehicle is able to transmit with a certain length of delay between successful BSM receptions. Notice that an IRT is measured in the number of time slots. It means that an IRT can also be measured in terms of the number of seconds by multiplying a slot time, $\mathsf{T}_{\text{slot}} = 50\ \mu$sec, as has been mentioned in Table 3. Intuitively speaking, applying the IEEE 1609.4 [25] as this paper assumes, each failed transmission takes an additional 100 msec since an entire beaconing period is wasted when an EXP occurs. This leads to an interpretation that the unit can always be translated to the length of time, i.e., 100 msec of IRT per beaconing period that is wasted.

In what follows, we discuss the implications of the results in detail. First, both PMF and CDF describe that the proposed scheme consumes fewer beaconing periods compared to the traditional CSMA, regardless of CW and N_{sta}. (We note that CDF is a better mark for observation of this statement.) The rationale behind the phenomenon is that the proposed multiple access mechanism yields a higher PDR as has been presented in Figure 6. We remind that the outperformance of the proposed scheme in terms of PDR is mainly attributed to a higher packet transmission probability, τ, as has been demonstrated in Figure 4.

Regarding the outperformance of the proposed scheme more specifically, Figure 7 also depicts that the margin of outperformance achieved by the proposed protocol gets greater with N_{sta} increased. This serves as a concrete evidence that the proposed scheme results in a higher efficiency as the DSRC network gets more congested.

Second, it is also suggested from both PMF and CDF that a larger N_{sta} leads to a higher probability of experiencing a longer IRT. The main reason of the tendency is a lower PDR that is induced by a higher P_{col} as N_{sta} is incremented.

Third, a larger CW yields a smaller IRT. Akin to the previous discussions, the relationship between IRT and CW is also attributed to PDR as has been presented in (8). That is, from Figure 6, one can find that a larger CW yields a

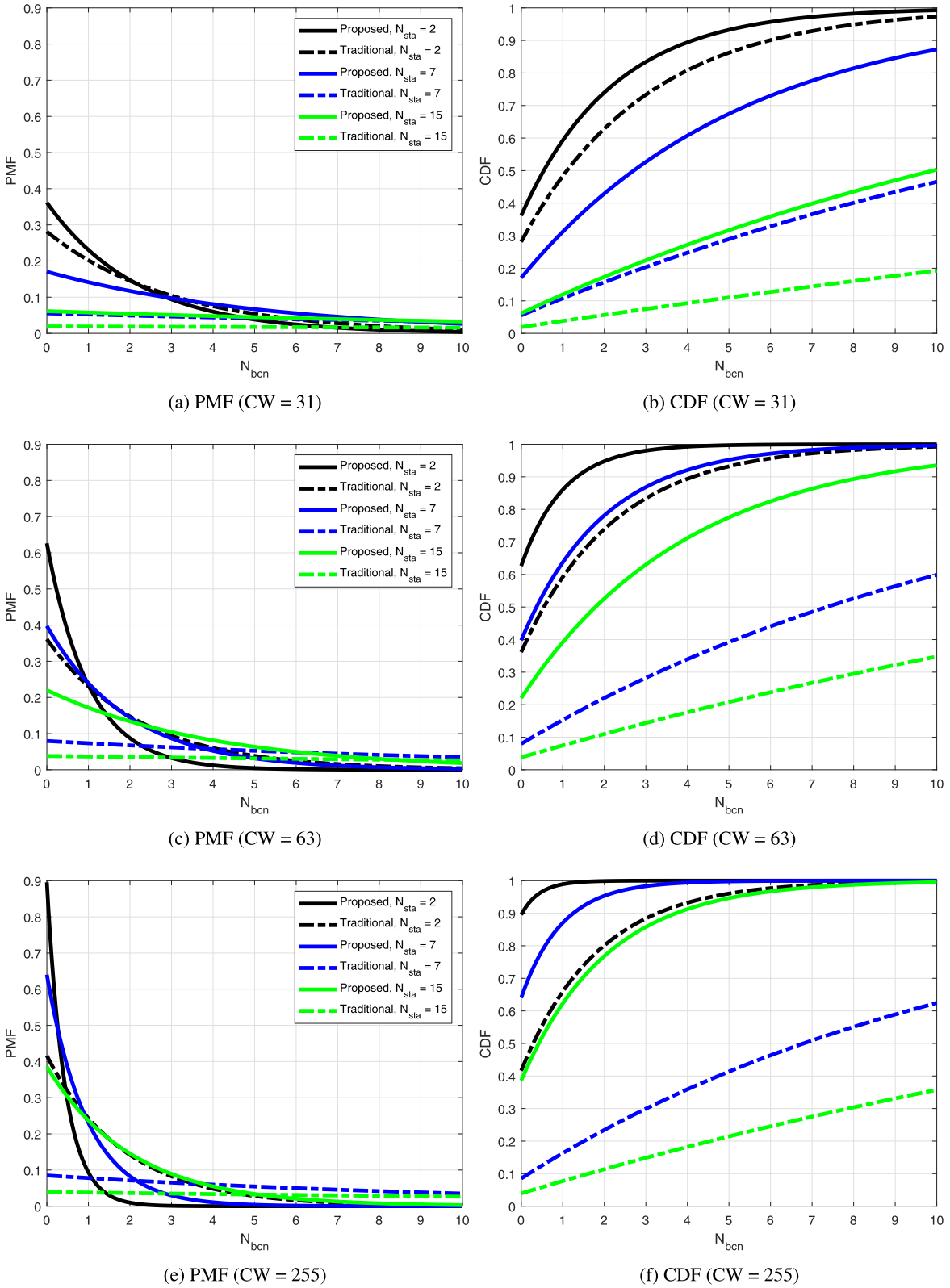

(a) PMF (CW = 31)

(b) CDF (CW = 31)

(c) PMF (CW = 63)

(d) CDF (CW = 63)

(e) PMF (CW = 255)

(f) CDF (CW = 255)

FIGURE 7. **Distribution of** IRT **(For CAT 1).**

higher PDR. As a direct consequence, the IRT gets lower as CW is increased, which is observed from comparison of CWs through 31, 63, and 255 in Figure 7.

VII. CONCLUSION

This paper proposed a protocol prioritizing the transmission of a BSM for a vehicle with a higher level of accident risk.

Our results showed that this protocol effectively improved the performance of vehicles with higher risk, measured in terms of key metrics–viz., average latency, throughput, and IRT. This paper also provided a generalized (i) analytical framework and (ii) spatial system model for evaluating the performance of the proposed scheme according to key factors such as the number of competing STAs and CW. We remind that the contribution of this paper is to lighten the networking load of a DSRC system. It will let DSRC suit better in coexistence scenarios with C-V2X, which are likely to happen considering that both of the two technologies have strengths that will have to be adopted in future connected vehicle networks.

Thanks to the generality, this work can be extended in multiple directions. For instance, based on the general model of node distribution (as opposed to previous work limiting the models to ''road'' environments), this paper's findings can be applied to other types of transportation network such as unmanned aerial vehicles (UAVs) for building a stochastic geometry-based framework analyzing latency and throughput performances.

It will be a meaningful attempt to extend this work if one (i) considers multiple factors potentially causing an accident and (ii) finds an explicit relationship among them to quantify the accident risk. For instance, it will be easy to identify a number of risk factors; but the hard part will be to characterize the exact impact on the accident risk as a result of the factors in concert.

REFERENCES

[1] United States Department of Transportation. (Jul. 2017). *Vehicle-to-Vehicle Communication Technology*. V2V Fact Sheet. [Online]. Available: https://www.nhtsa.gov/sites/nhtsa.dot.gov/files/documents/v2v fact sheet 101414 v2a.pdf

[2] X. Wang, S. Mao, and M. X. Gong, ''An overview of 3GPP cellular Vehicle-to-Everything standards,'' *GetMobile, Mobile Comput. Commun.*, vol. 21, no. 3, pp. 19–25, Nov. 2017.

[3] United States Department of Transportation. (Jul. 2015). *Status of the Dedicated Short-Range Communications Technology and Applications*. Report to Congress, FHWA-JPO-15-218. [Online]. Available: https://www.its.dot.gov/research_archives/connected_vehicle/pdf/DSRCReportCongress_FINAL_23NOV2015.pdf

[4] *Draft TGbd Comments on FCC NPRM Docket 19-138*, Standard IEEE P802.11, doc.: IEEE 802.11-20/0104r14, Feb. 2020. [Online]. Available: https://mentor.ieee.org/802.11/dcn/20/11-20-0104-00bd

[5] J. Kenney, ''An update on V2X in the United States,'' in *Proc. SIP-Adus Workshop Connected Automated Syst.*, Nov. 2018. [Online]. Available: https://www.sip-adus.go.jp/evt/workshop2018/file/new01_An_Update_on_V2X_in_the_United_States-Kenney-SIPadus-Nov.2018.pdf

[6] National Highway Traffic Safety Administration. *Proposed Rule Would Mandate Vehicle-to-Vehicle (V2V) Communication on Light Vehicles, Allowing Cars to 'Talk' to Each Other to Avoid Crashes*. NHTSA 34-16, Dec. 2016. [Online]. Available: https://one.nhtsa.gov/About-NHTSA/Press-Releases/ci.nhtsa_v2v_proposed_rule_12132016.print

[7] *In the Matter of Use of the 5.850-5.925 GHz Band*, document FCC 19-129, ET Docket 19-138, United States Federal Communications Commission, Washington, DC, USA, Dec. 2019.

[8] American Association of State Highway and Transportation Officials. (Aug. 2019). *State DOTs Sign Letter Supporting Preservation of 5.9 GHz Spectrum*. AASHTO J. [Online]. Available: https://aashtojournal.org/2019/08/23/state-dots-sign-letter-supporting-preservation-of-5-9-ghz-spectrum/

[9] S. Kim and M. Bennis, ''Spatiotemporal analysis on broadcast performance of DSRC with external interference in 5.9 GHz band,'' 2019, *arXiv:1912.02537*. [Online]. Available: http://arxiv.org/abs/1912.02537

[10] S. Kim and C. Dietrich, ''A novel method for evaluation of coexistence between DSRC and Wi-Fi at 5.9 GHz,'' in *Proc. IEEE Global Commun. Conf. (GLOBECOM)*, Dec. 2018, pp. 1–6.

[11] S. Kim and T. Dessalgn, ''Mitigation of civilian-to-military interference in DSRC for urban operations,'' in *Proc. MILCOM - IEEE Mil. Commun. Conf. (MILCOM)*, Nov. 2019, pp. 737–742.

[12] S. Kim, ''Impacts of mobility on performance of blockchain in VANET,'' *IEEE Access*, vol. 7, pp. 68646–68655, 2019.

[13] M. Haenggi, ''On distances in uniformly random networks,'' *IEEE Trans. Inf. Theory*, vol. 51, no. 10, pp. 3584–3586, Oct. 2005.

[14] A. K. Ligo, J. M. Peha, P. Ferreira, and J. Barros, ''Throughput and economics of DSRC-based Internet of vehicles,'' *IEEE Access*, vol. 6, pp. 7276–7290, 2018.

[15] A. I. Abu-Khadrah, Z. Zakaria, M. Othman, and M. S. I. M. Zin, ''Enhance the performance of EDCA protocol by adapting contention window,'' *Wireless Pers. Commun.*, vol. 96, no. 2, pp. 1945–1971, Apr. 2017.

[16] Y. S. Song and S. K. Lee, ''Analysis of periodic broadcast message for DSRC systems under high-density vehicle environments,'' in *Proc. Int. Conf. Inf. Commun. Technol. Converg. (ICTC)*, Oct. 2017, pp. 1008–1012.

[17] R. Zhang, F. Schmutz, K. Gerard, A. Pomini, L. Basseto, S. B. Hassen, A. Jaiprakash, I. Ozgunes, A. Alarifi, H. Aldossary, I. AIKurtass, O. Talabay, A. AlMhanna, S. AlGhamisi, M. AlSaleh, A. A. Biyabani, K. Al-Ghoneim, and O. K. Tonguz, ''Increasing traffic flows with DSRC technology: Field trials and performance evaluation,'' in *Proc. IECON - 44th Annu. Conf. IEEE Ind. Electron. Soc.*, Oct. 2018, pp. 6191–6196.

[18] Y. Liu, Z.-L. Wang, and B.-G. Cai, ''Investigation of a DSRC-based end of queue collision warning system by considering real freeway data,'' *IET Intell. Transp. Syst.*, vol. 13, no. 1, pp. 108–114, Jan. 2019.

[19] B. Cheng, H. Lu, A. Rostami, M. Gruteser, and J. B. Kenney, ''Impact of 5.9 GHz spectrum sharing on DSRC performance,'' in *Proc. IEEE Veh. Netw. Conf. (VNC)*, Nov. 2017, pp. 215–222.

[20] G. Wu and P. Xu, ''Improving performance by a dynamic adaptive success-collision backoff algorithm for contention-based vehicular network,'' *IEEE Access*, vol. 6, pp. 2496–2505, 2018.

[21] M. Ramakrishna, ''DBR: Distance based routing protocol for VANETs,'' *Int. J. Inf. Electron. Eng.*, vol. 2, no. 2, p. 228, 2012.

[22] S. Kim, ''A TDMA-based MAC between gateway and devices in M2M networks,'' in *Proc. IEEE Wireless Commun. Netw. Conf. Workshops (WCNCW)*, Apr. 2016, pp. 31–36.

[23] G. Lee, H. Kim, Y. Cho, and S.-H. Lee, ''QoE-aware scheduling for sigmoid optimization in wireless networks,'' *IEEE Commun. Lett.*, vol. 18, no. 11, pp. 1995–1998, Nov. 2014.

[24] *Dedicated Short Range Communications (DSRC) Message Set Dictionary*, Standard SAE J2735, SAE International, Apr. 2019.

[25] *IEEE Standard for Wireless Access in Vehicular Environments (WAVE)—Multi-Channel Operation*, Standard 1609.4-2016/Cor 1-2019, Sep. 2019.

[26] *IEEE Standard for Information technology-Local and metropolitan area networks-Specific requirements—Part 11: Wireless LAN Medium Access Control (MAC) and Physical Layer (PHY) Specifications Amendment 6:Wireless Access in Vehicular Environments*, Standard IEEE 802.11p, Jun. 2010.

[27] G. Bianchi, ''IEEE 802.11-saturation throughput analysis,'' *IEEE Commun. Lett.*, vol. 2, no. 12, pp. 318–320, Dec. 1998.

[28] P. Patel and D. K. Lobiyal, ''A simple but effective collision and error aware adaptive back-off mechanism to improve the performance of IEEE 802.11 DCF in error-prone environment,'' *Wireless Pers. Commun.*, vol. 83, no. 2, pp. 1477–1518, Jul. 2015.

[29] J. Edquist, C. M. Rudin-Brown, and M. G. Lenné, ''The effects of on-street parking and road environment visual complexity on travel speed and reaction time,'' *Accident Anal. Prevention*, vol. 45, pp. 759–765, Mar. 2012.

[30] C. Chen, N. Lù L. Liu, Q.-Q. Pei, and X.-J. Li, ''Critical safe distance design to improve driving safety based on vehicle-to-vehicle communications,'' *J. Central South Univ.*, vol. 20, no. 11, pp. 3334–3344, Nov. 2013.

[31] C. Campolo, Y. Koucheryavy, A. Molinaro, and A. Vinel, ''Characterizing broadcast packet losses in IEEE 802.11p/WAVE vehicular networks,'' in *Proc. IEEE 22nd Int. Symp. Pers., Indoor Mobile Radio Commun.*, Sep. 2011, pp. 735–739.

[32] R. Stanica, E. Chaput, and A.-L. Beylot, ''Reverse back-off mechanism for safety vehicular ad hoc networks,'' *Ad Hoc Netw.*, vol. 16, pp. 210–224, May 2014.

[33] X. Lei and S. H. Rhee, ''Performance analysis and enhancement of IEEE 802.11p beaconing,'' *EURASIP J. Wireless Commun. Netw.*, vol. 2019, no. 1, p. 61, Dec. 2019.

[34] W. Xu, H. Zhou, H. Wu, F. Lyu, N. Cheng, and X. Shen, "Intelligent link adaptation in 802.11 vehicular networks: Challenges and solutions," *IEEE Commun. Standards Mag.*, vol. 3, no. 1, pp. 12–18, Mar. 2019.
[35] M. Elwekeil, T. Wang, and S. Zhang, "Deep learning for joint adaptations of transmission rate and payload length in vehicular networks," *Sensors*, vol. 19, no. 5, p. 1113, Mar. 2019.
[36] S. Kim and B.-J. Kim, "Novel backoff mechanism for mitigation of congestion in DSRC broadcast," 2020, *arXiv:2005.08921*. [Online]. Available: http://arxiv.org/abs/2005.08921
[37] G. Bianchi, "Performance analysis of the IEEE 802.11 distributed coordination function," *IEEE J. Sel. Areas Commun.*, vol. 18, no. 3, pp. 535–547, Mar. 2000.

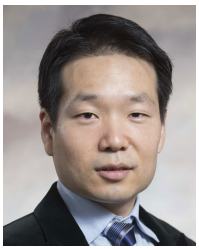

SEUNGMO KIM (Member, IEEE) received the B.S. and M.S. degrees in electrical communications engineering from the Korea Advanced Institute of Science and Technology (KAIST), Daejeon, South Korea, in 2006 and 2008, respectively, and the Ph.D. degree in electrical engineering from Virginia Tech, Blacksburg, VA, USA, in 2017. Since 2017, he has been an Assistant Professor with the Department of Electrical and Computer Engineering, Georgia Southern University, Statesboro, GA, USA. His current research interests include vehicle-to-everything (V2X) communications/networking, human exposure to electromagnetic field (EMF) in wireless systems, and coexistence of 5G and IEEE 802.11 in the 60 GHz band. He is a member of the IEEE Communications Society. He was a recipient of the Best Paper Award from the IEEE WCNC 2016 International Workshop on Smart Spectrum.

BYUNG-JUN KIM received the B.S. and M.S. degrees in statistics from Chung-Ang University, Seoul, South Korea, in 2013 and 2015, respectively, and the Ph.D. degree in statistics from Virginia Tech, Blacksburg, VA, USA, in 2020. He is currently an Assistant Professor with the Department of Mathematical Sciences, Michigan Technological University, Houghton, MI, USA. His current research interests include Bayesian functional estimation of multi-level time trend data with gas chromatography in analytical chemistry.